Amino Acids (2008) 34:539–545
DOI 10.1007/s00726-007-0007-4

ORIGINAL ARTICLE

Up-regulation of vimentin expression in low-density malignant glioma cells as immediate and late effects under irradiation and temozolomide treatment

Daniela Trog · Kristina Yeghiazaryan · Hans H. Schild · Olga Golubnitschaja

Received: 26 September 2007 / Accepted: 14 November 2007 / Published online: 29 November 2007

Abstract Nervous system tumors are one of the leading causes of cancer related death. Specific mechanisms facilitating the invasive behavior of gliomas remain obscure. Advanced simulation models of the in vivo response to therapy conditions should potentially improve malignant glioma treatment. Expressional profiling of vimentin—one of reliable pro-invasive tumor makers—in those simulation models was the goal of this study, in order to estimate a pro-invasive response of surviving malignant glioma cells under clinically relevant therapeutic conditions. Human U87-MG malignant glioma cells were used. These cells are characterized by the wild *p53*-phenotype, which is relevant for the majority of primary malignant glioblastomas. Experimental design foresaw the cells to undergo either irradiation or chemo-treatment with temozolomide alone, or combined treatment. Expression profiling of vimentin was performed by quantitative "Real-Time"-PCR under all treatment conditions simulating diverse tumor regions. Here we demonstrated that vimentin expression patterns in human malignant glioma cells strongly depend on cellular density, algorithms of drug delivery and chemo/radio treatment. Substantial differences were recognized between immediate and late therapy effects. Significant increase in vimentin expression levels was detected particularly in low-density cell cultures under durable treatment with constant concentration levels of temezolomide. Simulation of variable intratumoral regional conditions (central intratumoral regions vs. disseminated malignant cells in peripheral regions) demonstrated differential response of vimentin expression in malignant glioma cell cultures treated under clinically relevant conditions. Slight ebbing of expression levels as late effects of the treatment in confluent cultures may correspond to necrotic processes clinically observed in central intratumoral regions. Contrary, in disseminated malignant cells of peripheral regions therapy resulted in vimentin-inducing effects. This is in agreement with the clinical observations of an increased aggressiveness and malignancy grade of post-operatively chemo/radio-treated malignant gliomas.

Keywords Human malignant gliomas · Simulation of clinical glioma treatment · Temozolomide therapy · Pro-invasive molecular marker · Vimentin expression patterns

D. Trog · K. Yeghiazaryan · H. H. Schild · O. Golubnitschaja
Department of Radiology,
Friedrich-Wilhelms-University of Bonn,
53 105 Bonn, Germany

O. Golubnitschaja (✉)
Department of Radiology,
Division of Molecular/Experimental Radiology,
University of Bonn, Sigmund-Freud-Str. 25,
53 105 Bonn, Germany
e-mail: Olga.Golubnitschaja@ukb.uni-bonn.de

Introduction

Nervous system tumors are one of the leading causes of cancer related death. The diffusely infiltrative nature of malignant gliomas is the main obstacle to the successful surgical approach. Current post-operative therapy approaches, however, have minor success obviously due to sub-lethal effects as it has been recently shown (Trog et al. 2006a). Sub-lethal doses of irradiation are well-known to enhance the tumor invasiveness (Hegedus et al. 2004; Wild-Bode et al. 2001). Non-sufficient cell cycle control has been proposed as possible clue for the resistance of human malignant glioma cells to clinically relevant treatment conditions (Trog et al. 2007a).

Advanced bio-simulation methods are expected to substantially improve currently applied glioma treatments and patient-specific treatment planning. Optimized therapeutic algorithms are supposed to result in conformal shrinkage of tumors as well as in lowering of a potential invasiveness of the treated but, however, surviving malignant cells. The latter can be estimated by ex vivo/in vitro analysis of interplay among molecular pathways and even single biomarkers, which have been shown to be responsible for tumor invasiveness. In this work we investigated immediate and late molecular events, which accompany irradiation and chemo treatment in human malignant U87MG glioma cells. U87MG cell line is characterized by the wild *p53*-phenotype, which is relevant for the majority of primary malignant glioblastomas (Horiguchi et al. 2001). Highly up-regulated vimentin expression accompanied with a consequently growing malignancy grade of the surviving cell fractions have been recently demonstrated for U87MG cells (Trog et al. 2006b). This phenomenon is usually observed in later tumor reoccurrence after clinical gliomas treatment (Arab et al. 1999; Sallinen et al. 2000). Therefore, this cell line is considered to be suitable for in vitro simulation of clinically relevant treatments, estimation of pro-invasive molecular markers, and potential optimization of therapeutic algorithms.

The goal of the study was a comparative expression profiling of vimentin—the reliable marker of tumor invasiveness, in malignant glioma cells which survive under clinically relevant therapeutic algorithms. The non-sophisticated algorithms (see Fig. 1) have been recently published (Trog et al. 2007b) which simulate important intratumoral regional differences such as high intratumoral cell density compared to periphery as well as intracellular drug saturation depending on drug delivery and resistance. Short- as well as long-term effects on vimentin expression patterns are considered in the paper.

Materials and methods

Cell preparation and treatment

Human U87-MG glioma cells were cultured at 37°C in RPMI-1640 medium (Invitrogen, Scotland) supplemented

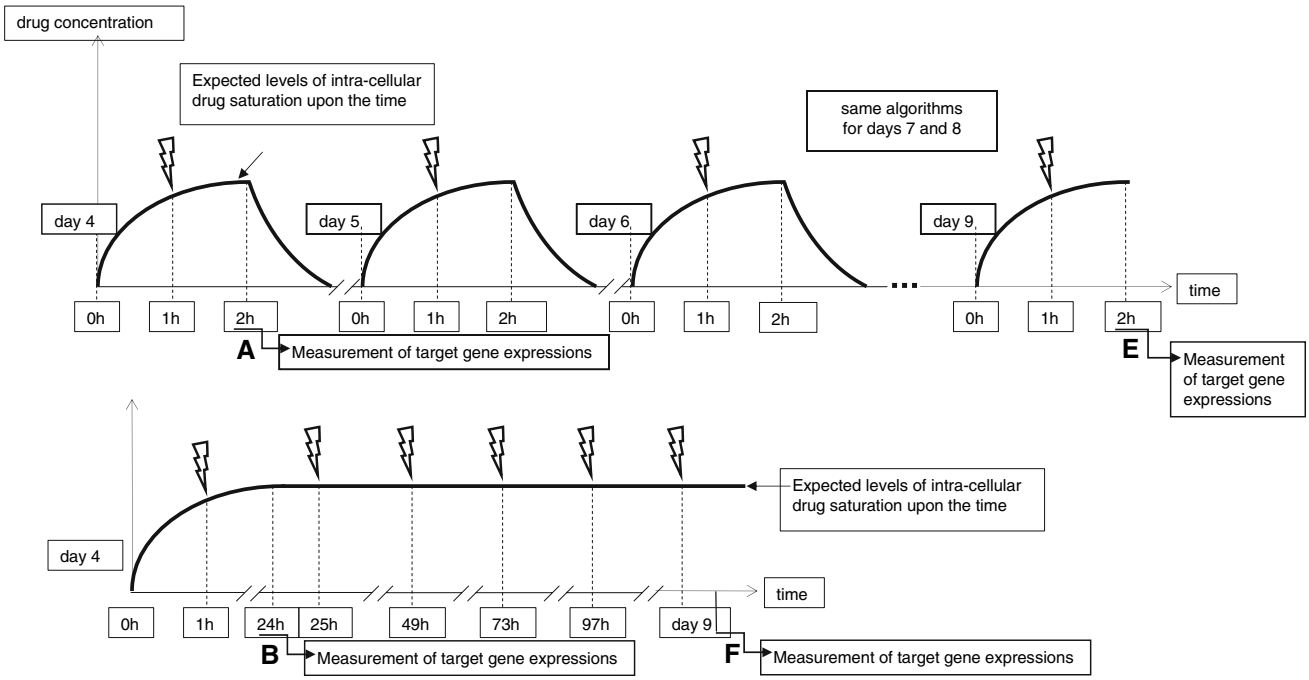

Fig. 1 Clinically relevant therapeutic algorithms applied to human malignant glioma cells (Trog et al. 2007b): In parallel experiments, the cells underwent chemo-treatment with 30 μg/ml of temozolomide (TMZ) in the cultivation medium combined with irradiation (2Gy, 200 KV x-ray, MG 420 Philips) according to the single algorithm A–F. The cases A and B simulated effects in peripheral intratumoral regions (i.e. disseminated single malignant cells outside of solid tumour) by using of non-confluent (low-density, day 4) cell cultures. Similarly, the algorithm C and D, however, simulated effects in central intratumoral regions by using of confluent (high-density) cell cultures: performed at day 9, C corresponds to A and D corresponds to B. Thereby, cases A and C analyzed immediate effects, whereas cases B and D analyzed late ones. Case E simulated immediate effects in peripheral intratumoral regions achieved by fluctuating intracellular saturation of TMZ as it is such in the case of pulsing drug delivery or fluctuating cellular drug efflux. Case F simulated long-term effects in peripheral intratumoral regions achieved by constant intracellular saturation of TMZ as it is such in the case of homogeneous well-targeted drug delivery

with 10% fetal calf serum (Invitrogen, Scotland) and 1% Penicillin/Streptomycin (Invitrogen, Scotland). In parallel experiments the cells underwent either irradiation (2Gy, 200 KV x-ray, MG 420 Philips) or chemo-treatment with 30 μg/ml of temozolomide in the cultivation medium, or combined chemo/radiation-treatment. The cell cultures were treated during 5 days from day 4 till day 9 of growth according to diverse clinically relevant therapeutic algorithms as given in Fig. 1. In order to simulate the fluctuating temozolomide concentration in algorithms E, medium containing temozolomide was daily replaced by medium without the drug—every time after 2-h chemo-treatment. As for the durable chemo-treatment under the algorithms B, D, and F, constant levels of temozolomide were kept during 24 h of treatment. Under the algorithm F medium containing temozolomide was refreshed every 24 h during 5 days of the treatment. By microscopic observations, non-confluent and confluent cultures were distinguished as described earlier (Trog et al. 2006a). Cell counting was performed using a Fuchs-Rosenthal counting cell chamber. After each treatment surviving cells were harvested, washed with PBS, aliquoted and stored at –80°C until expression analysis. All experiments were repeated three times for the proper statistical analysis.

Isolation of total RNA and mRNA

Total RNA was extracted using the commercial RNAzol-B isolation kit (WAK-Chemie Medical GmbH, Germany), and an isolation of mRNA from the individual total RNA-pools was performed using the Oligotex® mRNA Mini Kit (Qiagen, Germany) according to protocols supplied by the manufactures.

Reverse Transcriptase PCR (RT-PCR) and "Real-Time"-Quantitative PCR (RT-QPCR)

In order to detect the expression of target genes qualitatively and to optimize individual reaction conditions for concomitant RT-Quantitative PCR, reverse-transcriptase PCR was performed using specific primer-sets designed to β-actin (accession number X00351, positions 677–699 and 879–859 bp in cDNA) and vimentin (accession number M14144, positions 778–798 and 1064–1044 bp in cDNA).

Synthesized oligonucleotides had following sequences: for β-actin - 5′ TAAGGAGAAGCTGTGCTACG 3′ and 5′ TGAAGGTAGTTTCGTGGATG 3′and for vimentin 5′ GT TTCCAAGCCTGACCTCAC 3′ and 5′ GCTTCAACGGC AAAGTTCTC 3′ used as forward and reverse primers respectively. cDNA synthesis was performed using the "First-Strand cDNA Synthesis Kit" (GE Healthcare, UK). For each cDNA synthesis, 1 μg mRNA was reverse transcribed using the oligo(dT)18 primer in a final volume of 33 μl each, according to the protocol supplied by the manufacturer. After heat inactivation of reverse transcriptase 2 μl of the cDNA were used for each PCR-amplification. The PCR mixture contained 1 × PCR buffer (16.6 mmol/l ammonium sulfate, 67 mmol/l Tris, pH 8.8, 6.7 mmol/l $MgCl_2$, 10 mmol/l 2-mercaptoethanol), dNTPs (each at 1.25 mmol/l), primer pairs (100 pmol/l each per reaction), and cDNA-template in a final volume of 50 μl. Reactions were started at 95°C for 5 min before adding 1.5 units of Taq Polymerase (Red-Hot®, Thermo Fisher Scientific Inc, product line ABgene, UK) at the annealing temperature of 56°C followed by the polymerization at 72°C for 1 min. Amplification was carried out in a Perkin Elmer "DNA Thermal Cycler TC480" for 45 cycles (denaturation for 45 s at 95°C, annealing for 45 s at 56°C, and polymerization at 72°C for 30 s), followed by a final 7 min extension at 72°C. Negative controls without DNA as well as positive controls with a sequenced template were performed for each set of PCR experiments. PCR products (50 μl) were directly loaded onto 3% agarose gels ("Wide Range"—Agarose for analysis of DNA fragments longer than 50 bp, Sigma-Aldrich, USA), stained with ethidium bromide after electrophoresis, and directly visualized under UV illumination. The specificity of the amplification was controlled for each PCR product using site specific restriction analysis.

For the quantitative profiling of the target gene expression RT-QPCR was used. SYBR® Green I was utilized as the intercalation dye and fluorescent reporter molecule detecting the accumulation of the amplified double-stranded product in the iCycler iQIM Detection System (Bio-Rad, USA) according to the protocol supplied by manufacturer. An aliquot of 2 μl of the synthesized cDNAs was used for each RT-QPCR analysis. The reaction mixtures had the same contents as for RT-PCR with an exception of Red-Hot® polymerase (Thermo Fisher Scientific Inc, product line ABgene, UK) which was substituted for "Thermoprime Plus DNA Polymerase" from Thermo Fisher Scientific Inc, product line ABgene (UK), in order to avoid colour signal disturbances. The same optimized amplification program described above was also applied for quantitative real-time PCR analysis. The algorithm of the iCycler iQIM Detection System normalized the reporter signal (non-intercalated SYBR® Green I) to a passive reference and multiplies the SD of the background signal in the first few cycles by a default factor of 10, to determine a threshold (Heid et al. 1996). By subtracting the difference of the C_t values of the gene of interest from those of the housekeeping gene (β-actin), the data were normalized. The specificity of PCR amplification was controlled using the site specific restriction analysis of target PCR products. The amplification products underwent an

extraction from the agarose gel using DNA isolation kit (PEQLAB-Biotechnologie GmbH, Germany) before digestion. They were digested in a final volume of 50 µl with 20 units of each restriction endonuclease for 1 h, according to conditions specified by the manufacturer (Fermentas, Lithuania).

Statistical analysis

All statistical evaluations were done using the SPSS software (version 8.0). Statistical significance ($P < 0.05$) was calculated by the two-sided unpaired Student's *t*-test.

Results

Clinically relevant therapeutic algorithms applied to human malignant glioma cells are demonstrated in Fig. 1. Versus non-treated cell cultures at day 4 (non-confluent control) and day 9 (confluent control), following conditions for the combined chemo/radio treatment (RCT) were applied:

A. non-confluent (low-density) cell culture; molecular biological analysis was performed 1 h our after irradiation, when intra-cellular temozolomide saturation has been already reached; simulation of immediate effects in peripheral intratumoral regions;
B. non-confluent cell culture; molecular biological analysis was performed after one day of combined chemo/radio treatment; simulation of late effects in peripheral intratumoral regions;
C. confluent (high-density) cell culture; molecular biological analysis was performed 1 h our after irradiation, when intra-cellular temozolomide saturation has been already reached; simulation of immediate effects in central intratumoral regions;
D. confluent cell culture; molecular biological analysis was performed after one day of combined chemo/radio treatment; simulation of late effects in central intratumoral regions;
E. non-confluent cell culture, which, however, became confluent during the treatment; molecular biological analysis was performed after 5 days of combined chemo/radio treatment; simulation of effects achieved in peripheral regions by fluctuating intracellular saturation of TMZ in the case of pulsing drug delivery or fluctuating cellular drug efflux;
F. non-confluent cell culture, which remained non-confluent till the end of the treatment; molecular biological analysis was performed after 5 days of combined chemo/radio treatment; intra-cellular temozolomide saturation has been reached at the beginning and kept at the constant level till the end of the treatment; simulation of effects achieved in peripheral regions by homogeneous well-targeted drug delivery under prolonged combined chemo/radio treatment with constant intracellular saturation of TMZ.

Control cell cultures were analysed every day beginning with day 4 and finalizing with day 10. However, no significant differences in parameters measured have been observed at day 5 versus day 4 as well as at day 10 versus day 9. Therefore, additional data to days 5 and 10 are not presented in the manuscript. In parallel to the above described algorithms for the combined treatments, chemo- and radiation- treatments were applied also alone. In terms of cell culture confluence, similar cellular densities were observed, when the combined treatment and chemo-treatment alone were compared. In contrast, high cellular confluence comparable with that of non-treated cultures at day 9 was observed after durable application of irradiation alone (algorithms E and F).

In response to single treatment algorithms applied the corresponding regulation patterns of vimentin transcription rates are demonstrated in Fig. 2. Additionally, individual expression levels in treated cells relative to those of controls are summarized in Table 1. Expression levels in non-treated non-confluent cultures (control day 4) were 2,6-times lower compared to those in non-treated confluent cultures (control day 9). Noteworthy, compared to non-treated non-confluent cultures (control day 4) significant up-regulating effects were observed under all treatment conditions tested with the exception of those under algorithm E. Slight immediate and late up-regulating effects (algorithms A and B, respectively) were observed in treated non-confluent cell cultures. Thereby, almost equal (about two-times) up-regulating effects were achieved by radiation- and chemo-treatment alone as well as by the combined one.

Compared to non-treated confluent cells at day 9 decrease in vimentin expression rates was achieved under irradiation alone and combined treatment, when either algorithm E or F was applied. In contrast, when immediate and late effects in treated confluent cultures were considered (algorithms C and D), a significant expression up-regulation particularly by radiation and chemo treatment alone was observed.

Discussion

Malignant gliomas represent the most frequent brain malignancies which belong to human tumors with the worst prognosis. The diffuse character and disseminated growth of tumor periphery make a post-operative treatment of malignant gliomas especially complicate (see Fig. 3). It

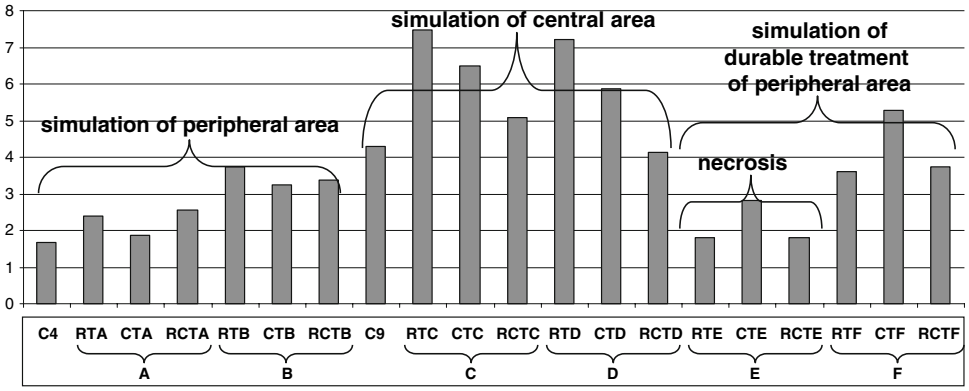

Fig. 2 Evaluation of vimentin mRNA expression patterns of non-treated (control) cells in non-confluent (C4, day 4) and confluent (C9, day 9) cultures as well as those of the cells treated according to algorithms A-F (see Fig. 1). *RTA* radiation treatment alone applied according to the algorithm A (see Fig. 1); *CTA* chemo-treatment alone applied according to the algorithm A; *RCTA* combined chemo/radio-treatment applied according to the algorithm A. Individual values represent a mean achieved in parallel experiments which was, further, normalized by corresponding expression level of β-actin as the house-keeping gene. RT, CT and RCT which belong to the same algorithm are shown as ligated together in the figure. Standard deviations for each mean value calculated were below 10% and, therefore, are not shown in the figure

Table 1 Differential expression of vimentin at the level of transcription in response to individual treatment algorithms (A–F)

	Relative to C4	Relative to C9
C9	2.55	
RT_A	1.42	
CT_A	1.11	
RCT_A	1.52	
RT_B	2.22	
CT_B	1.93	
RCT_B	2.01	
RT_C	4.44	1.74
CT_C	3.87	1.52
RCT_C	3.04	1.19
RT_D	4.29	1.68
CT_D	3.49	1.37
RCT_D	2.46	0.97
RT_E	1.07	0.42
CT_E	1.68	0.66
RCT_E	1.07	0.42
RT_F	2.15	0.84
CT_F	3.14	1.23
RCT_F	2.22	0.87

The values are given as a difference to those of non-treated (control) cells in non-confluent (C4, day 4) and confluent (C9, day 9) cultures

RT_A radiation treatment alone applied according to the algorithm A (see Fig. 1); *CT_A* chemo-treatment alone applied according to the algorithm A; *RCT_A* combined chemo/radio-treatment applied according to the algorithm A

has been clearly documented that current post-operative therapeutic approaches may even increase a degree of tumor malignancy and the potentially affected pathways

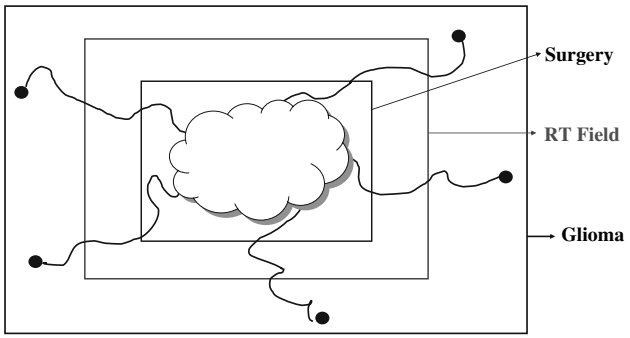

Fig. 3 Schematic representation of variable intratumoral regional conditions in malignant gliomas: central intratumoral regions versus disseminated malignant cells in peripheral regions. "Surgery", RT-field and "Glioma" localize operation-removable, radiation-treated and glioma-affected regions, respectively. The diffuse character and disseminated growth of tumor periphery make a post-operative treatment of malignant gliomas especially complicate

regulating pro-invasive molecular events have been considered (Trog et al. 2006a, b).

Recent works demonstrated in vivo and ex vivo significant differences in regional molecular expression and even differential regional contrast enhancement in malignant gliomas that may highly affect a local treatment response (van Meter et al. 2006; Provenzale et al. 2006). Advanced in vitro simulation methods are expected to substantially improve currently applied therapy forms and should lead to optimal therapeutic planning for individual patients as well as development of novel therapeutic targets. According to our recently published work on in vitro modeling of clinically relevant therapeutic algorithms (Trog et al. 2007b), here we simulated potentially variable intratumoral regional conditions and differentiated between:

- high versus low cellular density of malignant glioma cells
- simple versus combined chemo/radio-treatment
- repeated pulsing versus continued drug delivery that corresponds to fluctuating versus permanent intracellular drug saturation, respectively
- immediate (early) versus late treatment response at the level of basic gene expression regulation (mRNA)
- molecular effects in peripheral versus central intratumoral regions under treatment conditions used.

The results clearly demonstrated substantial differences in all points listed above. Earlier we have already reported a significant increase in vimentin protein expression demonstrated by proteomics approaches in malignant glioma cells which undergo either temozolomide-treatment alone or combined with irradiation, if compared to non-treated cells with relatively low basal vimentin expression (Trog et al. 2006b). These data are well in agreement with those observed in the current work at the level of transcription, when algorithm F is considered. The current work aimed additionally at detailed study of early and late vimentin regulating effects under further conditions considering plenty of clinically relevant situations.

Vimentin belongs to the group of glioma specific extracellular matrix components, which are associated with invading tumour cells and vascular elements that clarify and emphasise the overlapping biological function of vimentin in both neo-vascularization and invasion of malignant glial cells. In our experiments we observed an additional up-regulation of vimentin expression as immediate and late effects under irradiation and temozolomide treatment in low-density malignant glioma cells. Particularly, vimentin-conveying effects were observed under durable treatment with permanent concentration levels of temozolomide (algorithm F). Noteworthy, fluctuating temozolomide concentration levels had decreasing effects on vimentin expression (algorithm E). Slight ebbing of expression levels as late effects of the treatment in confluent cultures may correspond to necrotic processes clinically observed in central intratumoral regions. In central regions neither immediate nor late effects of combined chemo/radio treatment on vimentin expression were monitored.

An extensive vimentin expression is known to be typical for highly infiltrative gliomas with poor prognosis (Dehghani et al. 1998; Mahesparan et al. 2003), and has been postulated as a molecular marker for astrocytomas with enhanced motility and higher invasive potential (Rutka et al. 1999). Our current result, therefore, strongly supports the clinical observations of an increased aggressiveness and malignancy grade of post-operatively chemo/radio-treated malignant gliomas.

Concluding remarks

Our proof-of-principle study simulated potentially variable intratumoral regional conditions and demonstrated differential basic regulation of vimentin in malignant glioma cell cultures treated under clinically relevant conditions. The main message of this works is that effects which might be achieved by treatment of central intratumoral regions cannot be expected in disseminated malignant cells in peripheral regions. The most unfavorable effects in terms of potential therapy failure were demonstrated in disseminated glioma cells. This result strongly supports the clinical observations of an increased aggressiveness and malignancy grade of post-operatively chemo/radio-treated malignant gliomas.

References

Arab S, Rutka J, Lingwood C (1999) Verotoxin induces apoptosis and the complete, rapid, long-term elimination of human astrocytoma xenografts in nude mice. Oncol Res 11:33–39

Dehghani F, Schachenmayr W, Laun A, Korf HW (1998) Prognostic implication of histopathological, immunohistochemical and clinical features of oligodendrogliomas: a study of 89 cases. Acta Neuropathol 95:493–504

Hegedus B, Zach J, Czirok A, Lovey J, Vicsek T (2004) Irradiation and Taxol treatment result in non-monotonous, dose-dependent changes in the motility of glioblastoma cells. J Neurooncol 67:147–157

Heid CA, Stevens J, Livak KJ, Williams PM (1996) Real time quantitative PCR. Genome Res 6:986–994

Horiguchi H, Sano T, Hirose T (2001) TP53 deleted cells in de novo glioblastomas using fluorescence in situ hybridization. Pathol Int 51:187–192

Mahesparan R, Read T A, Lund-Johansen M, Skaftnesmo KO, Bjerkvig R, Engebraaten O (2003) Expression of extracellular matrix components in a highly infiltrative in vivo glioma model. Acta Neuropathol 105:49–57

Provenzale JM, York G, Moya MG, Parks L, Choma M, Kealey S, Cole P, Serajuddin H (2006) Correlation of relative permeability and relative cerebral blood volume in high-grade cerebral neoplasms. AJR Am J Roentgenol 187:1036–1042

Rutka JT, Ivanchuk S, Mondal S, Taylor M, Sakai K, Dirks P, Jun P, Jung S, Becker LE, Ackerley C (1999) Co-expression of nestin and vimentin intermediate filaments in invasive human astrocytoma cells. Int J Dev Neurosci 17:503–515

Sallinen SL, Sallinen PK, Haapasalo HK, Helin HJ, Helen PT, Schraml P, Kallioniemi OP, Kononen J (2000) Identification of differentially expressed genes in human gliomas by DNA microarray and tissue chip techniques. Cancer Res 60:6617–6622

Trog D, Yeghiazaryan K, Fountoulakis M, Friedlein A, Moenkemann H, Haertel N, Schueller H, Breipohl W, Schild H, Leppert D, Golubnitschaja O (2006a) Pro-invasive gene regulating effect of irradiation and combined temozolomide-radiation treatment on surviving human malignant glioma cells. Eur J Pharmacol 542:8–15

Trog D, Fountoulakis M, Friedlein A, Golubnitschaja O (2006b) Is current therapy of malignant gliomas beneficial for patients? Proteomics evidence of shifts in glioma cells expression patterns under clinically relevant treatment conditions. Proteomics 6:2924–2930

Trog D, Moenkemann H, Breipohl W, Schueller H, Schild H, Golubnitschaja O (2007a) Non-sufficient cell cycle control as possible clue for the resistance of human malignant glioma cells to clinically relevant treatment conditions. Amino Acids 32:373–379

Trog D, Yeghiazaryan K, Schild H, Golubnitschaja O (2007b) Pro-invasive molecular events in human malignant glioma cells strongly depend on algorithm of chemo/radio treatment, cellular density, and drug delivery. Eur J Pharmacol (accepted)

van Meter T, Dumur C, Hafez N, Garrett C, Fillmore H, Broaddus WC (2006) Microarray analysis of MRI-defined tissue samples in glioblastoma reveals differences in regional expression of therapeutic targets. Diagn Mol Pathol 15:195–205

Wild-Bode C, Weller M, Rimner A, Dichgans J, Wick W (2001) Sublethal irradiation promotes migration and invasiveness of glioma cells: implications for radiotherapy of human glioblastoma. Cancer Res 61:2744–2750